Int. J. Electrochem. Sci., 8 **(2013)** 12884 - 12893

International Journal of
ELECTROCHEMICAL
SCIENCE
www.electrochemsci.org

Extract of *Momordica charantia* (Karela) Seeds as Corrosion Inhibitor for P110SS Steel in Co_2 Saturated 3.5% NaCl Solution

Ambrish Singh[1,2], *Yuanhua Lin*[1,*], *Wanying Liu*[1], *Eno. E. Ebenso*[3], *Jie Pan*[4]

[1] State Key Laboratory of Oil and Gas Reservoir Geology and Exploitation (Southwest Petroleum University), Chengdu, Sichuan 610500, China.
[2] Department of Chemistry, School of Civil Engineering, LFTS, Lovely Professional University, Phagwara, Punjab, India.
[3] Material Science Innovation & Modelling (MaSIM) Focus Area, Faculty of Agriculture, Science and Technology, North-West University (Mafikeng Campus), Private Bag X2046, Mmabatho 2735, South Africa
[4] CNPC Key Lab for Tubular Goods Engineering (Southwest Petroleum University), Chengdu, Sichuan 610500, China.
[*]E-mail: yhlin28@163.com

Received: 18 August 2013 / *Accepted:* 29 September 2013 / *Published:* 20 October 2013

The inhibition behavior of *Momordica charantia* seeds (MCS) as an eco-friendly corrosion inhibitor for P110SS steel was investigated in 3.5 wt.% NaCl saturated with CO_2 solution by means of polarization curve, AC impedance, and scanning electrochemical spectroscopy (SECM). The results showed that MCS can inhibit the corrosion of P110SS steel. The maximum inhibition efficiency is achieved when MCS concentration is 1000 ppm by weight in this study. The adsorption of the studied inhibitor obeyed the Langmuir's adsorption isotherm.

Keywords: P110SS steel; Inhibitor, Corrosion; EIS; SECM

1. INTRODUCTION

Carbon dioxide (CO_2) corrosion is one of the major problems in oil and gas industry, costing billions of dollars every year [1]. Due to its low cost and availability, steel is used as the primary construction material for pipelines in oil and gas industries, but it is very susceptible to corrosion in CO_2 environments. Aqueous carbon dioxide (carbonic acid) is corrosive and corrodes the carbon steel pipelines. Carbon dioxide corrosion has been of interest to researchers in oil industries for many years and there exists many theories about the mechanism of CO_2 corrosion [2]. The mechanisms of CO_2

corrosion and the formation and removal of protective iron carbonate films are not fully understood due to the complex reaction mechanisms and the presence of many critical environmental factors such as pH, temperature, dissolved species concentration and hydrodynamics that can appreciably change the corrosion rate.

Use of corrosion inhibitors is the most common method used to retard corrosion of metals as no special equipments required, low cost and easy operation. Overall, many corrosion inhibitors have some health and/or environmental problems due to their toxicity. It is highly desired that new inhibitors for Al are non-toxic and environment-friendly. Use of different parts of plant as corrosion inhibitor is in practice nowadays as they are renewable, cheap, easily available and non toxic. Many amines, steroids and alkaloids are derived from the plants which are rich in heteroatoms (N, O, S). Mostly, compounds containing heteroatoms show good inhibition studies [4-6].

Momordica charantia often called bitter melon, bitter gourd or bitter squash in English, has many other local names. Goya from the indigenous language of Okinawa and karavella from Sanskrit are also used by English-language speakers. It is a tropical and subtropical vine of the family Cucurbitaceae, widely grown in Asia, Africa, and the Caribbean for its edible fruit, which is extremely bitter. Its many varieties differ substantially in the shape and bitterness of the fruit. Bitter melon comes in a variety of shapes and sizes. The cultivar common to China is 20–30 cm long, oblong with bluntly tapering ends and pale green in color, with a gently undulating, warty surface. The plant contains several biologically active compounds, chiefly momordicin I and momordicin II, and cucurbitacin B. The plant also contains several bioactive glycosides (including momordin, charantin, charantosides, goyaglycosides, momordicosides) and other terpenoid compounds (including momordicin-28, momordicinin, momordicilin, momordenol, and momordol). It also contains cytotoxic (ribosome-inactivating) proteins such as momorcharin and momordin [6-11].

In present study we have investigated *MCS* as corrosion inhibitor of P110SS steel in 3.5% NaCl solution using electrochemical and scanning electrochemical spectroscopy.

2. EXPERIMENTAL

2.1. Preparation of inhibitor

Fifty grams of dried *Momordica charantia* plant seeds were soaked in 900 ml of reagent grade ethanol for 24 h and refluxed for 5 h. The ethanolic solution was filtered and concentrated to 500 ml. This extract was used to study the corrosion inhibition properties.

2.2. Materials and Solutions

P110SS steel having the following chemical composition (wt %): C 0.27; Si 0.26; Mn 0.6; P 0.009; S 0.003; Cr 0.5; Ni 0.25; Mo 0.6; Nb 0.05; V 0.005; Ti 0.02; Fe balance were used for all studies. P110SS steel coupons having dimensions of 30 mm × 3 mm × 3 mm were used for the electrochemical study. The specimens were metallographically polished according to ASTM A262, degreased and dried before experiment. The test solution of 3.5% NaCl was prepared by analytical grade NaCl with double distilled water. All experiments were performed at room temperature.

2.3. Electrochemical measurements

The electrochemical experiments were performed by using three electrode cell, connected to Potentiostat/Galvanostat AUTOLAB model GSTAT302N. Software package incorporated with AUTOLAB was used for data fitting. P110SS steel was used as working electrode, platinum electrode as an auxiliary electrode, and saturated calomel electrode (SCE) as reference electrode. All potentials reported were measured versus SCE. Tafel curves were obtained at a scan rate of 1.0 mVs^{-1}. EIS measurements were performed under potentiostatic conditions in a frequency range from 100 kHz to 0.01 Hz, with amplitude of 10 mV AC signal. The experiments were carried out when the electrochemical system was in steady state in 3.5% NaCl saturated with CO_2 in absence and presence of different concentrations of MCS.

2.4. Scanning Electrochemical Microscopy (SECM)

A model of scanning electrochemical microscopy CHI900C was used. The instrument was operated with a 10 μm platinum tip as the probe, an Ag/AgCl/KCl (saturated) reference electrode and a platinum counter electrode. The tip and substrate are part of an electrochemical cell that usually also contains other (e.g., auxiliary and reference) electrodes. All potential values are referred to the Ag/AgCl/KCl (saturated) reference electrode. The measurements of line scans were generated with the tip at ~ 10 μm from the specimen surface in all the cases. The scan rate was 80 μm/step. The diameter of the samples was between 30 × 3 × 3 mm.

3. RESULTS AND DISCUSSION

3.1. Electrochemical measurements

3.1.1. Potentiodynamic polarization measurements

The corrosion potential (E_{corr}), corrosion current density (I_{corr}), and anodic (β_a) and cathodic (β_C) slopes are obtained by the anodic and cathodic regions of the tafel plots shown in table 1.

Table 1. Tafel polarization data for P110SS steel in 3.5% NaCl at different concentration of MCS.

Solutions	Tafel data						
	Conc.(ppm)	E_{corr} (V vs. SCE)	I_{corr} (A cm^{-2}) (V d^{-1})	b_a (V d^{-1})	b_c (%)	η%	θ
3.5% NaCl		-0.6	9.82	0.05	0.86	-	-
MCS	250 ppm-0.6	6.40	0.10	0.57	34	0.34	
MCS	500 ppm-0.7	3.52	0.09	0.12	64	0.64	
MCS	1000 ppm	-0.7	1.01	0.08	0.18	89	0.89

The corrosion current density (I_{corr}) can be obtained by extrapolating the tafel lines to the corrosion potential and the inhibition efficiency (η %) values were calculated from the relation:

$$\eta\% = \frac{I_{\text{corr}} - I_{\text{corr(i)}}}{I_{\text{corr}}} \times 100 \qquad (1)$$

Where I_{corr} and $I_{\text{corr(i)}}$ are the corrosion current density in absence and presence of inhibitor. The polarization curves for P110SS steel in the absence and presence of the inhibitor are given in figure 1.

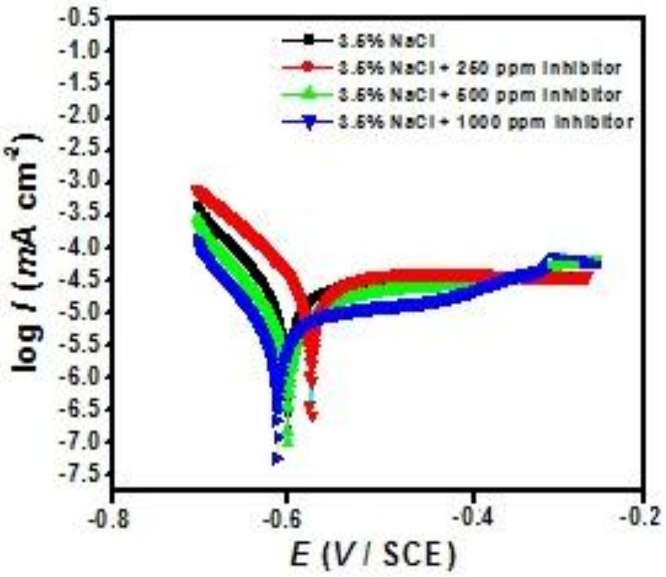

Figure 1. Tafel polarization plots for P110SS steel in absence and presence of MCS.

The results showed the decrease in I_{corr} in presence of inhibitor as compared to blank solution this is due to adsorption of inhibitor on metal surface which penetrates rate of corrosion current density and increases inhibition efficiency [12-15]. But, analysis of both anodic (b_a) and cathodic (b_c) tafel slope values indicated that both anodic and cathodic reactions were suppressed during the addition of the inhibitor, which suggested that the MCS reduced anodic dissolution and also retarded the hydrogen evolution reaction. The addition of MCS do not alter the value of E_{corr} which was not more than 85 mV as compare to blank 3.5% NaCl indicating the mixed type of inhibiting behaviour of the added inhibitor [16-20].

3.1.2. Electrochemical Impedance Spectroscopy

Electrochemical impedance spectroscopy measurements were carried out in order to study the kinetics of the electrode process and the surface properties of the studied system. This method is widely used to investigate the corrosion inhibition process [21, 22]. Nyquist plots of P110SS steel in 3.5% NaCl solution in the absence and presence of different concentrations of MCS are shown in figure 2.

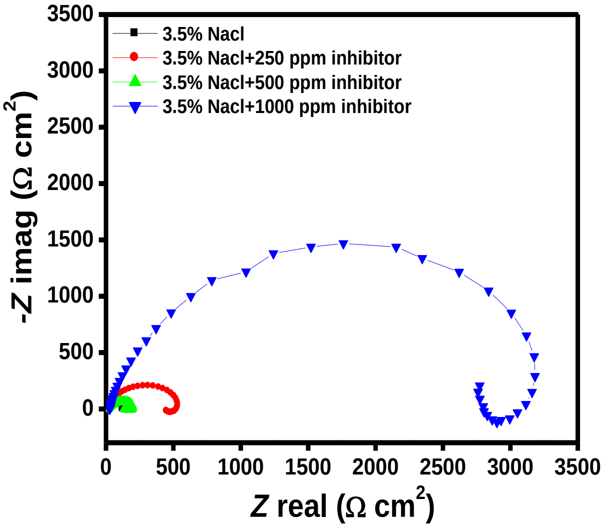

Figure 2. Nyquist plots for P110SS steel in absence and presence of MCS.

However, after the addition of MCS, the impedance modulus of the system gradually increased and was a maximum in the case of MCS. The impedance diagram (Nyquist) contains depressed semicircles with the center under the real axis with one capacitive loop in the high frequency (HF) zone, and one RL − L inductive loop in the lower frequency (LF) zone. As usually indicated in an EIS study, the HF capacitive loop is related to the charge-transfer resistance (Rct = Rp-Rs) process of the metal corrosion and the double-layer behavior, and these loops are not perfect semicircles. Such behavior is characteristic for solid electrodes and is often referred to as a frequency dispersion effect which can be imputed to non homogeneity and the rough-textured metal surface. The LF inductive loop may be a consequence of the layer stabilization byproducts of the corrosion reaction on the electrode involving inhibitor molecules and their reactive products [23, 24]

The model used for fitting consist of R_s (the resistance of solution between working electrode and counter electrode), R_{ct}, inductive elements L, RL and the constant phase angle element (CPE) as shown in figure 3.

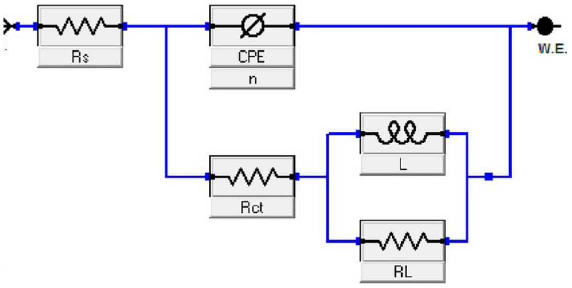

Figure 3. Equivalent circuit used to fit the Nyquist curves.

The inhibition efficiency is calculated using charge transfer resistance (R_{ct}) as follows,

$$\eta\% = \frac{R_{\text{ct(inh)}} - R_{\text{ct}}}{R_{\text{ct(inh)}}} \times 100 \qquad (2)$$

Where $R_{\text{ct(inh)}}$ and R_{ct} are the values of charge transfer resistance in presence and absence of inhibitor in 3.5% NaCl respectively. At different concentrations MCS showed increase in value of R_{ct} with respect to blank 3.5% NaCl solution. The increase in R_{ct} values as shown in table 2 is attributed due to increase in resistance and adsorption of inhibitor molecules on P110SS steel surface [25-27].

Table 2. Nyquist data for P110SS steel in 3.5% NaCl at different concentration of MCS.

Solutions	Conc.(ppm)	R_s (Ω cm^2)	R_{ct} (Ω cm^2)	η%	θ	n
3.5% NaCl	-	3.4	154	-	-	0.851
MCS	250 ppm	5.4	189	18	0.18	0.816
MCS	500 ppm	3.8	627	75	0.75	0.869
MCS	1000 ppm	4.6	3036	94	0.94	0.887

3.2. Adsorption isotherm

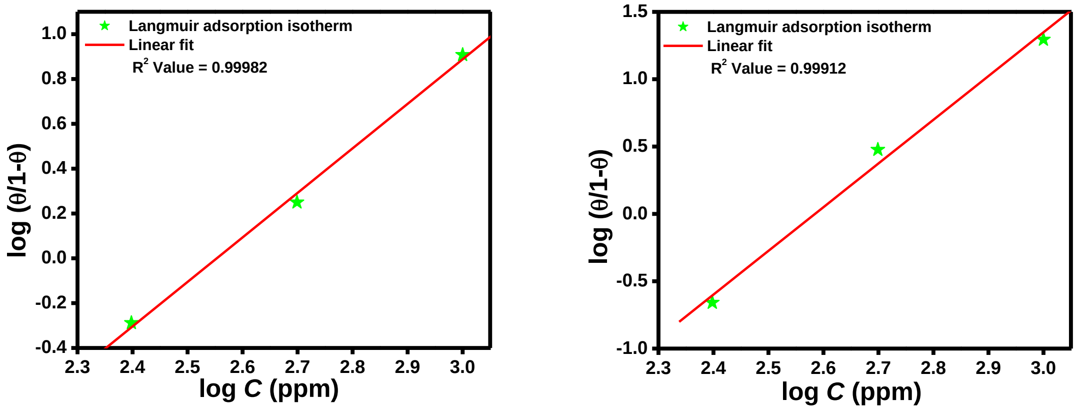

(a) **(b)**

Figure 4. The Langmuir adsorption isotherm plots for mild steel at different concentrations of MCS by (a) Tafel and (b) EIS method.

The adsorption of an organic adsorbate on to metal-solution interface can be represented by a substitutional adsorption process between the organic molecules in the aqueous solution phase ($\text{Org}_{\text{(sol)}}$) and the water molecules on the metallic surface ($H_2O_{\text{(ads)}}$) [28].

$$\text{Org}_{\text{(sol)}} + xH_2O \rightarrow \text{Org}_{\text{(ads)}} + xH_2O_{\text{(sol)}} \qquad (3)$$

where, x is the size ratio representing the number of water molecules replaced by one molecule of organic adsorbate. Basic information on the interaction between the inhibitor and the P110SS steel surface can be provided by the adsorption isotherm. It is essential to know the mode of adsorption and the adsorption isotherm that can give important information on the interaction of inhibitor and metal surface. The linear regression coefficient values (R^2) determined from the plotted curve of Langmuir was found to be in the range of 0.99982 for tafel and linear regression coefficient values (R^2) for EIS was 0.99912 (figure 4).

$$\theta = \frac{bC_{inh}}{1+bC_{inh}} \quad \text{(Langmuir Isotherm)} \quad (4)$$

3.3. Surface Analysis

3.3.1. Scanning Electrochemical Microscopy

The scanning electrochemical microscope (SECM) [29] has been introduced to the corrosion field, giving valuable microscopic information from a corroding surface [30, 31] allowing the measurement of local differences in electrochemical reactivity. The important advantage of the SECM technique is that it operates on both insulating (coated / films) and conducting (non-coated) surfaces, thus allowing one to easily distinguish between the coated and corroded surfaces [32]. Figure 5a-h presents the morphology of the specimens visualized by scanning electrochemical microscope in presence and absence of MCS. The status of a corroded sample was studied by monitoring the probe (tip potential: 0.5 V vs Ag/AgCl/saturated KCl reference electrode) and the substrate (tip potential: -0.7 V) in test solutions. Corrosion activity is observed from 10 minutes after immersion in the electrolyte solution.

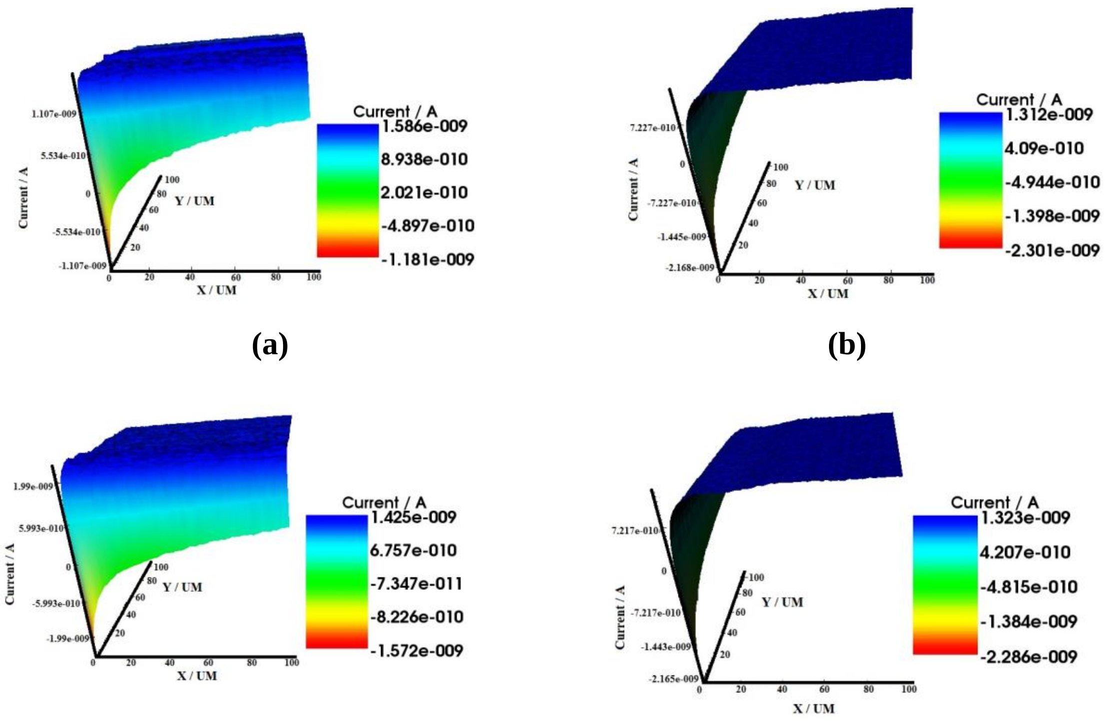

(a) **(b)**

(c) **(d)**

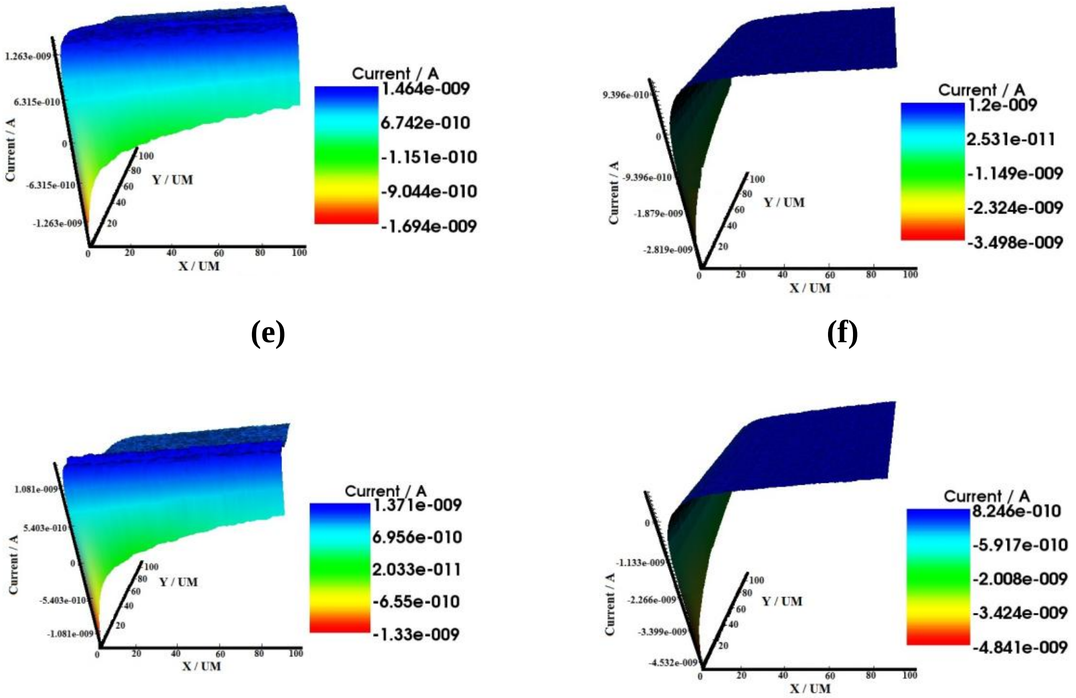

(e) **(f)**

(g) **(h)**

Figure 5. SECM images of P110SS steel in 3.5% NaCl (a) x-axis 3-D view (b) y-axis 3-D view and MCS (c) 250 ppm x-axis 3-D (d) 250 ppm y-axis 3-D (e) 500 ppm x-axis 3-D (f) 500 ppm y-axis 3-D (g) 1000 ppm x-axis 3-D (h) 1000 ppm y-axis 3-D

When an insulating surface (having film or coating) as we used different concentration of MCS with 3.5% NaCl solution is approached in an SECM measurement the diffusion field surrounding the tip is hindered and the tip current decreases as shown in table 3.

Table 3. SECM data of blank 3.5% NaCl x-axis, y-axis and inhibited x-axis, y-axis at optimum concentration (1000 ppm) of MCS.

	Blank 3.5% NaCl		MCS 1000 ppm	
Sr. no.	x-axis Current (A)	y-axis Current (A)	x-axis Current (A)	y-axis Current (A)
1.	1.107e-09	7.227e-10	1.081e-09	0
2.	5.534e-10	0	5.403e-10	-1.133e-09
3.	0	-7.227e-10	0	-2.266e-09
4.	-5.534e-10	-1.445e-09	-5.403e-10	-3.399e-09
5.	-1.107e-09	-2.168e-09	-1.081e-09	-4.532e-09

This is typical for an insulating surface. On the contrary, an increase in the current is observed when a conductor blank 3.5% NaCl solution without MCS is approached, because the redox mediator is regenerated at the surface. In the absence of MCS the P110SS steel surface remains conductive, which are evidenced by an increase in current as the surface is approached. When MCS has been added to the solution a gradual transition from a conducting to an insulating surface is seen. Comparing the currents across the corroded sample and the specimens incorporated with inhibitor solution, the protection effect of the inhibitor adsorbed on the specimen surface can be vindicated [33].

4. MECHANISM OF ADSORPTION AND INHIBITION

The adsorption process is affected by the chemical structures of the inhibitors, the nature and charged surface of the metal and the distribution of charge over the whole inhibitor molecule [34]. Due to the complex nature of adsorption and inhibition of a given inhibitor, it is impossible for single adsorption mode between inhibitor and metal surface. Since there are many chemical constituents in MCS so they may inhibit the P110SS steel surface due to the synergism between them. Another possibility is that the large size of the glycosides covers the entire surface thereby reducing corrosion.

The inhibition process of P110SS steel in the studied environment can be explained by the adsorption of the components of MCS on the metal surface. MCS constitutes of glycosides, oils, fatty acids, saponins which are very rich in heteroatoms (N, O), which meet the general consideration of typical corrosion inhibitors. The adsorption of these compounds on metal surface reduces the surface area that is available for the attack of the aggressive ion from the 3.5% NaCl solution [35-38]. The inhibition of P110SS steel corrosion in 3.5% NaCl solutions by MCS extract can also be explained on the basis of electrochemical results obtained from EIS curves which clearly showed the increase in R_{ct} values on addition of the inhibitor as compared to blank. From the polarization results, it is evident that MCS extract inhibit the corrosion by controlling both the anodic and cathodic reactions. All these data are in good agreement with each other.

5. CONCLUSIONS

In this study, corrosion inhibition efficiency of MCS on P110SS steel in 3.5% NaCl was determined by electrochemical and surface analysis. The potentiodynamic polarization data indicated that the MCS were of mixed type. Electrochemical impedance spectroscopy data reveals increase in R_{ct} values which accounted for good inhibition efficiency. The adsorption of the inhibitor molecules on the P110SS steel surface was found to obey the Langmuir adsorption isotherm. The surface studies by scanning electrochemical spectroscopy confirmed the blockage of metal surface through adsorption process. All these data support good inhibition tendency of MCS.

ACKNOWLEDGEMENTS

Research work was co-financed by the National Natural Science Foundation of China (No. 51274170) and the research grants from the Colonel Technology Fund of Southwest Petroleum University (Project No.2012XJZ013). Without their support, this work would not have been possible.

References

1. D. G. Li, Y. R. Feng, Z. Q. Bai, M. S. Zheng, *Appl. Surf. Sci.* 253 (2007) 8371.
2. K. Bilkova, E. Gulbrandsen, *Electrochim. Acta*. 53 (2008) 5423.
3. Ambrish Singh, E.E. Ebenso, M. A. Quraishi, *Int. J. Electrochem. Sci.* 7 (2012) 3409.
4. M. A. Quraishi, A. Singh, V. K. Singh, D. K. Yadav, A.K. Singh, *Mater. Chem Phys.* 122(2010) 114.
5. Ambrish Singh, I. Ahamad, V. K. Singh, M. A. Quraishi, *J. Solid State Electr.* 15 (2011) 1087.
6. M. Fatope, Y. Takeda, H. Yamashita, H. Okabe, T. Yamauchi, *J. Natur. Pdts.* 53 (1990) 1491.
7. S. Begum, M. Ahmed, B. S. Siddiqui, A. Khan, Z. S. Saify, M. Arif, *Phytochem.* 44 (1997) 1313.
8. H. Okabe, Y. Miyahara, T. Yamauci, *Chem. Pharmaco. Bull.* 30 (1982) 4334.
9. Y. Kimura, T. Akihisa, N. Yuasa, M. Ukiya, T. Suzuki, M. Toriyama, S. Motohashi, H. Tokuda, *J. Natur. Pdts.* 68 (2005) 807.
10. Chi-I; Chang, Chiy-Rong; Chen, Yun-Wen; Liao, Hsueh-Ling; Cheng, Yo-Chia; Chen, Chang-Hung Chou, *J. Natur. Pdts.* 71 (2008) 1327.
11. Toshihiro; Akihisa, Naoki; Higo, Harukuni; Tokuda, Motohiko; Ukiya, Hiroyuki; Akazawa, Yuichi; Tochigi, Yumiko; Kimura, Takashi Suzuki, *J. Natur. Pdts.* 70 (2007) 1233.
12. G. Ji, S. K. Shukla, P. Dwivedi, S. Sundaram, R. Prakash, *Ind. Eng. Chem. Res.* 50 (2011) 11954.
13. I. Ahamad, R. Prasad, M. A. Quraishi, *J. Solid State Electrochem.* 14 (2010) 2095.
14. Ambrish Singh, I. Ahamad, V. K. Singh, M. A. Quraishi, *Chem. Engg. Comm.* 199 (2012) 63.
15. N. O. Eddy, S. R. Stoyanov, Eno E. Ebenso, *Int. J. Electrochem. Sci.* 5 (2010) 1127.
16. M. Lebrini, F. Robert, A. Lecante, C. Roos, *Corros. Sci.* 53 (2011) 687.
17. A. Singh, V. K. Singh, M. A. Quraishi, *Int. J. Corros.* doi:10.1155/2010/275983.
18. D. K. Yadav, M. A. Quraishi, B. Maiti, *Corros. Sci.* 55 (2011) 254.
19. Ambrish Singh, Eno E. Ebenso, M.A. Quraishi, *Int. J. Electrochem. Sci.* 7 (2012) 4766.
20. Husnu Gerengi, Halil Ibrahim Sahin, *Ind. Eng. Chem. Res.* 51 (2012) 780.
21. I. B. Obot, E.E. Ebenso, Zuhair M. Gasem, *Int. J. Electrochem. Sci.* 7 (2012) 1997.
22. Nnabuk O. Eddy, Femi E. Awe, Abdulfatai A. Siaka, Ladan Magaji, Eno E. Ebenso, *Int. J. Electrochem. Sci.* 6 (2011) 4316.
23. K. F. Khaled, *Electrochim. Acta* 55 (2010) 5375.
24. D. K. Yadav M. A. Quraishi, *Ind. Eng. Chem. Res.* 51 (2012) 14966.
25. S. Deng, X. Li, *Corros. Sci.* 55 (2012) 407.
26. S. Banerjee, V. Shrivatsava, M. M. Singh, *Corros. Sci.* 59 (2012) 35.
27. P.B. Raja, A.A. Rahim, H. Osman, K. Awang, *Int. J. Miner. Metall. Mater.* 18 (2011) 413.
28. R. Solmaz, G. Kardas, M. Culha, B. Yazici, M. Erbil, *Electrochim. Acta* 53 (2008) 5941.
29. A. J. Bard, F. R. F. Fan, J. Kwak, O. Lev, *Anal. Chem. 61* (1989) 132.
30. C. Lee, J. Kwak, A. J. Bard, *Proc. Natl. Acad. Sci. USA, 87* (1990) 1740.
31. S. Amemiya, Z. Ding, J. Zhou, A. J. Bard, *J. Electroanal. Chem.* 7 (2000) 483.
32. F. R. F. Fan, A. J. Bard, *J. Phys. Chem. B.* 106, (2002) 279.
33. C. G. Zoski, B. Liu, A. J. Bard, *Anal. Chem.* 76 (2004) 3646.
34. I. O. M. Bockris, B. Yang, *J. Electrochem. Soc.* 138 (2012) 2237.
35. P. B. Raja, A. K. Qureshi, A. A. Rahim, H. Osman, K. Awang, *Corros. Sci.* 69 (2013) 292.
36. A. Khamis, M. M. Saleh, M. I. Awad, *Corros. Sci.* 66 (2013) 343.
37. P. B. Raja, M. Fadaeinasab, A. K. Qureshi, A. A. Rahim, H. Osman, M. Litaudon, K. Awang, *Ind. Eng. Chem. Res.* 52 (2013) 10582.
38. Ambrish Singh, I. Ahamad, M. A. Quraishi, *Arab. J. Chem.* (2012) http://doi.dx.10.1016/j.arabjc.2012.04.029.